Relationship between Chemical Composition and M_s Temperature in High-Entropy Shape Memory Alloys

L. Peltier[1] · F. Meraghni[1] · S. Berveiller[1] · P. Lohmuller[2] · P. Laheurte[2]

Abstract Five high entropy alloys with shape memory effect or superelastic effect were prepared by cold crucible melting to understand the effect of their chemical composition on the transformation temperatures. The microstructure and phases of the alloys at room temperature were investigated by optical and scanning electron microscopy. The calorimetric study of these alloys is employed to analyze the reversible transformation from austenite to martensite and to determine the transformation temperatures of the five alloys. The paper presents the results of several published works relating the transformation temperatures of high entropy shape memory alloys (HE-SMA). An experimental database has been built up to understand the influence of the different alloying elements and their related concentrations on the transformation temperature M_s (Martensite Start) of the HE-SMAs. An equation is identified using the database to predict the transformation temperature M_s of a high entropy shape memory alloy as a function of its weighted chemical composition, which exhibits a metallurgical solutioned treatment (ST) state and a specific mixing entropy ($\Delta Smix/R$) range.

Keywords High entropy alloy · Shape memory alloy · Superelasticity · Shape memory effect · Martensitic transformation · M_s temperature prediction

✉ L. Peltier
laurent.peltier@ensam.eu

[1] LEM3, Arts et Métiers Institute of Technology, Université de Lorraine, CNRS, HESAM Université, 4 rue Augustin Fresnel, 57070 Metz, France

[2] LEM3, Université de Lorraine, Arts et Métiers Institute of Technology, CNRS, 7 rue Félix Savart, 57070 Metz, France

Introduction

The alloy composition has been used as the most important parameter to determine approximatively the transformation temperature of shape memory alloys (SMAs) [1–4]. Several empirical equations have been proposed to rely on the chemical composition to the M_s temperature. However, differences in transformation temperature in an identical composition can be observed [5] and [6] or for alloys with composition ranges out of bounds from those used to formulate the equations. Indeed, transformation temperatures can be modified by heat treatments [7], microstructure [8] and work hardening rate [9]. Because of the interaction of multiple factors and processing conditions, it is necessary to analyze the dependence of the transformation temperatures on the alloying composition. It is useful to get a first accurate approximation of the transformation temperature ranges as a function of the chemical composition when designing an alloy towards its improvement, especially for the multicomponent system. The purpose of this study is to understand the effect of the alloying elements of HE-SMAs on their martensite transformation temperature and to establish a relationship between them that can provide an accurate prediction prior to the stage of the alloy manufacturing. Most of the alloys studied in this work are in the same homogenized metallurgical state (Solutioned Treatment or ST).

Experimental Procedure and Database Set-Up

Eighteen HE-SMAs alloys studied in the literature were analyzed in terms of M_s temperature to build an experimental database from published work or previous works of the authors. Five alloys are obtained using a cold crucible

Table 1 Experimental database providing chemical compositions of the studied alloys (at. % and wt. %) and the corresponding M_s temperature determined by DSC

Authors			Composition at. %											Composition wt. %										Ms
			Ti	Hf	Zr	Nb	Ta	Fe	Co	Al	Cu	Pd	Ni	Ti	Hf	Zr	Nb	Ta	Fe	Co	Al	Cu	Pd	Ni	(°c)
Abuzaid	2018	[24]	2.50					42.50	15.00	10.00			30.00	2.21					43.89	16.35	4.99			32.56	-80
Canadinc	2019	[14]	16.67	16.67	16.67							25.00	25.00	8.50	31.60	16.10							28.20	15.60	525
Chang	2019	[32]	16.67	16.67	16.67						5.00		45.00	9.67	36.05	18.43						3.85		32.00	350
Chang	2019	[32]	16.67	16.67	16.67						15.00		35.00	9.61	35.84	18.32						11.48		24.75	245
Chang	2019	[32]	16.67	16.67	16.67						25.00		25.00	9.56	35.63	18.21						19.03		17.57	175
Chen	2019	[31]	16.67	16.67	16.67				10.00		15.00		25.00	9.50	35.50	18.33				7.30		11.70		17.70	100
Chumlyakov	2020	[23]	2.50					41.00	17.00	11.50			28.00	2.23					42.68	18.67	5.78			30.63	-100
Li	2019	[16]	25.00	15.00	10.00						25.00		25.00	15.50	34.10	12,00						19.60		18.80	-70
Peltier	2020	[13]	16.00	19.00	15.00						23.00		27.00	8.90	39.60	16.00						17.00		18.50	200
Peltier	2021	[19]	30.00	19.00	25.00	13.00	13.00							13.50	31.80	21.40	11.30	22.00							-17
$Ni_{50.6}Ti_{49.4}$-like	Present work		21.83	11.45	16.17						31.44		19.11	13.60	26.60	19.20						26.00		14.60	-110
$Ni_{50}Ti_{50}$-like	Present work		16.67	16.67	16.67				7.50		17.50		25.00	9.60	35.81	18.30				5.31		13.36		17.63	198
$Ti_{77}Nb_{23}$-like	Present work		25.00	19.00	33.00	17.00	6.00							11.70	33.00	29.33	15.49	10.50							100
Wang	2019	[15]	50.00	15.00	20.00	5.00				10.00				31.40	35.10	22.00	7.90				3.60				600
Yaacoub	2020	[5]	16.67	16.67	16.67				10.00		15.00		25.00	9.60	35.80	18.30				7.10		11.50		17.70	157
Zhang	2019	[21]				2.00		44.00	16.50	10.00			27.50				3.40		44.70	17.70	4.90			29.30	-100

The database consists of experimental results of 16 HE-SMAs: 11 alloys from the open literature, 2 from previous works by the authors and 3 alloys specifically cast for this study

to complete this work and validate the equation expressing the M_s temperature of HE-SMAs as a function of their chemical compositions. Among the five alloys specifically manufactured for this study only three have been utilized to enrich the database presented in Table 1. These three HE-SMAs are: $Ni_{50.6}Ti_{49.4}$-like alloy, $Ni_{50}Ti_{50}$-like alloy and $Ti_{77}Nb_{23}$-like alloy and referred to as Present Work in Table 1.

It is worth mentioning that the compositions of prepared alloys are determined using a scanning electron microscope (SEM) by energy-dispersive X-ray spectrometry technique (EDX) as shown in Fig. 1a, b and c. Furthermore, phase transformation temperatures are studied using the differential scanning calorimetry technique (DSC) in Fig. 2. The transformation temperatures between the martensite and the austenite (M_s, M_f, A_s and A_f) are determined using dedicated software. Samples of the alloys produced for the study have a mass of around 40 mg according to ASTM [10]. To ensure the ST state of the prepared DSC samples previously obtained by cutting, a specific heat treatment has been performed under Argon gaseous protection at 1000 °C for 30 min, then 900 °C for 10 min and finally quenched in water at room temperature according to ASTM F2004. This heat treatment has been achieved within a homemade device developed specifically for small DSC samples ensuring hence their ST state. Chemical compositions and representative microstructures of $Ni_{50.6}Ti_{49.4}$-like alloy, $Ni_{50}Ti_{50}$-like alloy and $Ti_{77}Nb_{23}$-like (at. %). produced alloys are presented in Fig. 1. The choice of these three alloys is motivated by the large range of their M_s temperatures contrasting between -100 °C and 200 °C, as shown in their respective thermograms in Fig. 2.

The M_s temperatures of the other studied HE-SMAs are summarized in Table 1. It is important to emphasize that the whole HE-SMAs presented in the database have different types and different chemical compositions: NiTi-like [5, 11–18], TiNb-like [19], NiAl-like [20, 21], CuAl-like [22] and FeAl-like [23, 24]. In addition, it should be noted that all the alloys selected to enrich the database, either specifically developed for the study or taken from the open literature, are in the same metallurgical state (Solution Treatment or ST).

Results and Discussion

As early as the 1970s, Ahlers et al. [1] proposed an empirical equation linking the chemical composition to the transformation temperature of a ternary CuZnAl alloy. This linear function is the result of data extracted from 25 different alloys. Belkala et al. did the same for a CuAlBe system [25, 26], Recarte et al. for a CuAlNi system [27]. More recently, Frentzel et al. has studied the effect of Ni content (at. %) in the TiNi binary system [4]. Kim and Miyazaki have been interested in determining the M_s of TiNb alloys [3]. Over the past fifty years, the SMAs family has expanded, notably with the SMAs with high entropy branch (HE-SMAs). It is worth emphasizing that this paper aims at proposing and validating a relationship linking the chemical composition with the M_s temperature of this new class of alloys, namely the HE-SMAs. Piorunek et al. [17] have already provided a similar relationship for calculating the M_s temperature of HE-SMAs. They compared the

Fig. 1 SEM and EDX analyses of three manufactured alloys: **a** $Ni_{50.6}Ti_{49.4}$-like alloy, **b** $Ti_{77}Nb_{33}$-like alloy, **c** $Ni_{50}Ti_{50}$-like alloy

$Ni_{50.6}Ti_{49.4}$-like

Elements	at. %	wt. %
Ti	21.83	13.60
Hf	11.45	26.60
Zr	16.17	19.20
Nb		
Ta		
Fe		
Co		
Cu	31.44	26.00
Ni	19.11	14.60
Ti-like	49.45	59.40
Ni-like	50.55	40.60
ΔSmix/R	1.55	
Ms Exp (°C)	-110	

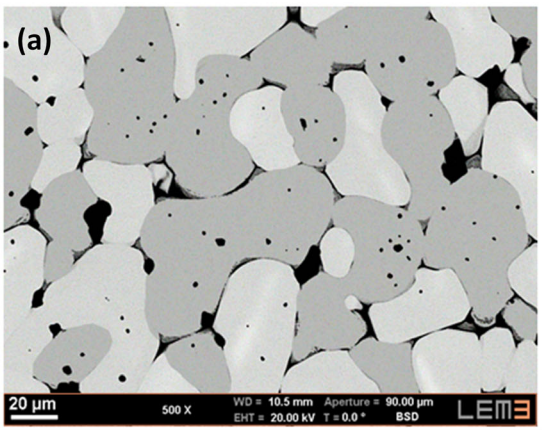

$Ti_{77}Nb_{23}$-like

Elements	at. %	wt. %
Ti	25.00	11.70
Hf	19.00	33.00
Zr	33.00	29.33
Nb	17.00	15.49
Ta	6.00	10.50
Fe		
Co		
Cu		
Ni		
Ti-like	77.00	74.03
Ni-like	23.00	25.97
ΔSmix/R	1.50	
Ms Exp (°C)	100	

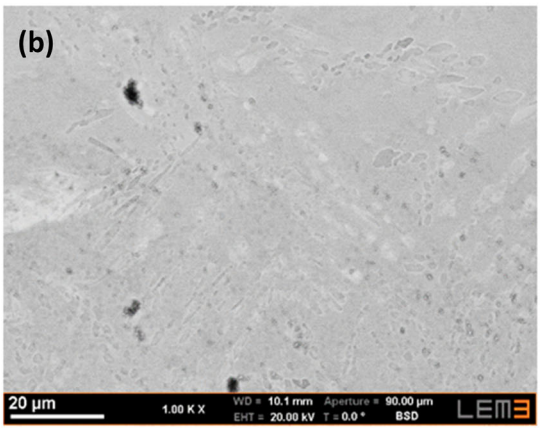

$Ni_{50}Ti_{50}$-like

Elements	at. %	wt. %
Ti	16.67	9.60
Hf	16.67	35.81
Zr	16.67	18.30
Nb		
Ta		
Fe		
Co	7.50	5.30
Cu	17.50	13.36
Ni	25.00	17.63
Ti-like	50.01	63.71
Ni-like	49.99	36.29
ΔSmix/R	1.74	
Ms Exp (°C)	198	

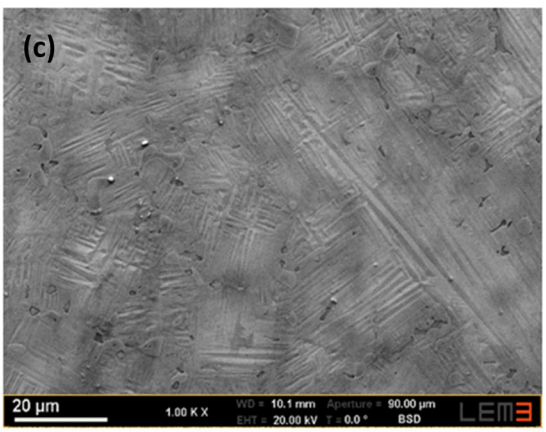

results with the various studies of Frentzel et al. [4] on binary TiNi alloys.

In the present paper, a relationship has been identified using the database of the alloys presented in Table 1. The latter has been built by considering several metallurgical features of the HE-SMAs alloys. The first aspect deals with the metallurgical state. Indeed, all the HE-SMAs studied are in the solution treated (ST) homogenized state. So, each composition is unique and results in a single transformation temperature M_s in the database. The published works by Piorunek et al. [11, 17] show indeed that for the same composition, the M_s transformation temperature evolves according to the stages of solution treatment of the intermetallics. It should be pointed out in this paper all the studied alloys are assumed to be homogenized and the contribution of the intermetallics is neglected since it does not exceed 5% as stated in our previous work [28]. The second aspect is related to the specific mixing entropy

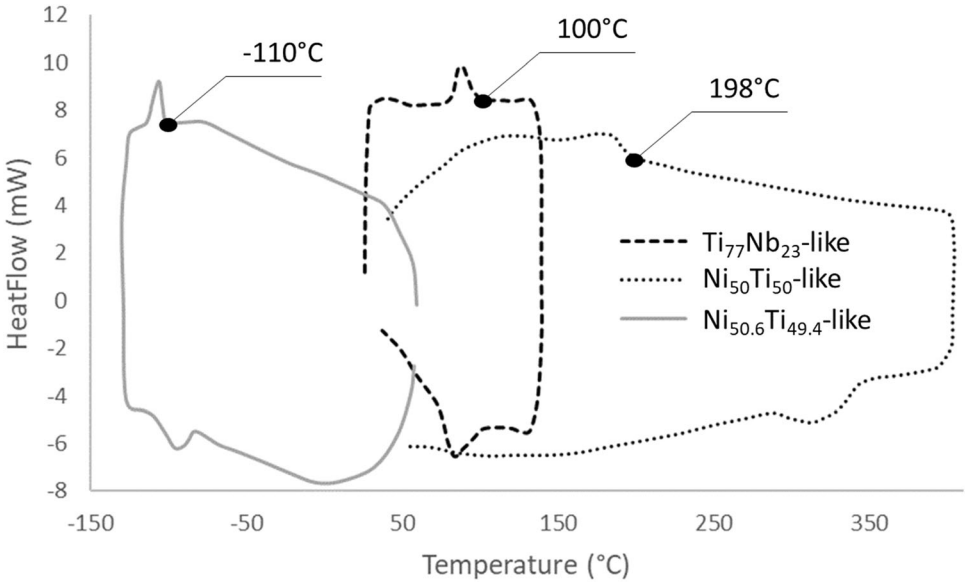

Fig. 2 Thermograms obtained through DSC analyses for the three manufactured alloys $Ni_{50.6}Ti_{49.4}$-like alloy, $Ni_{50}Ti_{50}$-like alloy and $Ti_{77}Nb_{23}$-like alloy

(ΔSmix/R), ranging between 1.3 and 1.75, where R is the gas constant [29, 30]. In fact, Piorunek et al. [11] shows that for the same NiTi-like composition, there are differences between the M_s temperatures of low entropy binary alloys and the quinary or even the senary alloys with high entropy. These differences between the M_s temperatures confirm that one cannot use the same equation for calculating the M_s temperatures of the NiTi-like compositions since the M_s depends on the number of the constitutive elements and their related ponderation in terms of weight concentrations, which corresponds to the criterion of the mixing entropy (ΔSmix/R). However, it must be pointed out that the metallurgical states of the NiTi-like alloys produced by Piorunek et al. [17] have not been homogenized ST state and consequently they are not reported in Table 1. Besides, several other papers investigated alloys whose compositions were identical, but they do not have the same temperatures Ms. In fact, for example, $(TiHfZr)_{50}Ni_{25}Co_{10}Cu_{15}$ was studied by Firstov et al. [6] with a M_s temperature of 155 °C since it was not in a homogenized ST state whereas Chen et al. [31] as well Yaacoub et al. [5] investigated the same alloy in homogenized ST state and found respectively a M_s temperature of 36 °C and of 13 °C, which are comparable. The alloy $(TiHfZr)_{50}(NiCu)_{50}$ was studied by Chang et al. [32] finding that its M_s temperature was 197 °C but Firstov et al. [12] found for the same quinary alloy in a non-homogenized state a M_s temperature of 255 °C. Although these alloys have the same composition, the differences in terms of M_s are related to their metallurgical states. Consequently, only the results regarding the homogenized ST state of these two alloys have been reported in Table 1 and considered in the database of the present work.

By considering the alloys that exhibit homogenized ST states and a specific mixing entropy (ΔSmix/R) ranging between 1.3 and 1.75, one can build:

1. A matrix C_{ij} providing the concentration (wt. %) of an alloying element (j) in the analyzed alloy (i). Equation (1) shows the concentration matrix $C(16, 11)$ built as a rectangular matrix of 16 arrows corresponding to the analyzed studied alloys: 11 alloys taken from the open literature, 2 from previous works by the authors and 3 alloys cast for this study (all the references are summarized in Table 1). The 11 columns of the matrix represent the alloying elements.

$$C = \begin{array}{c} \begin{bmatrix} Ti & Hf & Zr & Nb & Ta & Fe & Co & Al & Cu & Pd & Ni \end{bmatrix} \\ \begin{bmatrix} 13.60 & 26.60 & 19.20 & 0 & 0 & 0 & 0 & 0 & 26.00 & 0 & 14.60 \\ 2.23 & 0 & 0 & 0 & 0 & 42.68 & 18.67 & 5.78 & 0 & 0 & 30.63 \\ 0 & 0 & 0 & 3.40 & 0 & 44.70 & 17.70 & 4.90 & 0 & 0 & 29.30 \\ 2.21 & 0 & 0 & 0 & 0 & 43.89 & 16.35 & 4.99 & 0 & 0 & 32.56 \\ 15.50 & 34.10 & 12.00 & 0 & 0 & 0 & 0 & 0 & 19.60 & 0 & 18.80 \\ 13.50 & 31.80 & 21.40 & 11.30 & 22.00 & 0 & 0 & 0 & 0 & 0 & 0 \\ 9.50 & 35.50 & 18.33 & 0 & 0 & 0 & 7.30 & 0 & 11.70 & 0 & 17.70 \\ 11.70 & 33.00 & 29.33 & 15.49 & 10.50 & 0 & 0 & 0 & 0 & 0 & 0 \\ 9.60 & 35.80 & 18.30 & 0 & 0 & 0 & 7.10 & 0 & 11.50 & 0 & 17.70 \\ 9.56 & 35.63 & 18.21 & 0 & 0 & 0 & 0 & 0 & 19.03 & 0 & 17.57 \\ 9.60 & 35.81 & 18.30 & 0 & 0 & 0 & 5.31 & 0 & 13.36 & 0 & 17.63 \\ 8.90 & 39.60 & 16.00 & 0 & 0 & 0 & 0 & 0 & 17.00 & 0 & 18.50 \\ 9.61 & 35.84 & 18.32 & 0 & 0 & 0 & 0 & 0 & 11.48 & 0 & 24.75 \\ 9.67 & 36.05 & 18.43 & 0 & 0 & 0 & 0 & 0 & 3.85 & 0 & 32.00 \\ 8.50 & 31.60 & 16.10 & 0 & 0 & 0 & 0 & 0 & 0 & 28.20 & 15.60 \\ 31.40 & 35.10 & 22.00 & 7.90 & 0 & 0 & 0 & 3.60 & 0 & 0 & 0 \end{bmatrix} \end{array} \quad (1)$$

2. A vector (M_s^{Exp})i consisting of the 16 values of M_s temperature (°C) of the studied alloys HEA in homogenized ST states, which have been determined experimentally by 13 different authors or in 2 previous papers by the authors as well as the M_s temperature of the three alloys investigated in the present work, namely: $Ni_{50}Ti_{50}$-like, $Ni_{50.6}Ti_{49.4}$-like, $Ti_{77}Nb_{23}$-like (at. %). The M_s^{Exp} vector is given in Eq. 2.

$$M_s^{Exp} = \begin{bmatrix} -110 \\ -100 \\ -100 \\ -80 \\ -70 \\ -17 \\ 100 \\ 100 \\ 157 \\ 175 \\ 198 \\ 200 \\ 245 \\ 350 \\ 525 \\ 600 \end{bmatrix} \quad (2)$$

One can formulate then an overdetermined system of linear equations as follows:

$$C_{ij}.p_j = (M_s^{Exp})_i \quad \begin{matrix} i = 1, 2, ..., 16 \\ j = 1, 2, ..., 11 \end{matrix} \quad (3)$$

(p_j) $j = 1, 2, ..., 11$ is a vector containing the ponderation coefficients (°C.(wt. %)-1) of the concentration for the element (j) that has to be determined (unknowns) by solving the previous overdetermined system (1). The Eq. (3) is solved using the pseudo-inverse technique [33] since the matrix C_{ij} cannot be inverted. The solution (p_j) is then estimated by solving the following system equation:

$$C_{ji} \cdot C_{ij} \cdot p_j = C_{ji} \cdot (M_s^{Exp})_i \quad (4)$$

The Equation system (4) can be written using the matrix notation as:

$$^T[C] \cdot [C] \cdot \{p\} = {}^T[C] \cdot \{M_s^{Exp}\} \quad (5)$$

The solution of the Eq. (5) is then:

$$\{p\} = \left[{}^T[C] \cdot [C]\right]^{-1} {}^T[C] \cdot \{M_s^{Exp}\} \quad (6)$$

The Eq. (6) provides the vector (p) that is directly computed using matrix algebra via Matlab® software.

For an alloy, the Eq. (7) expresses then the evolution of the martensite temperature (M_s^{Calc} (°C)) predicted as a function of its chemical composition (Table 1) considering the ponderation coefficient (weighted alloying element composition). It reads:

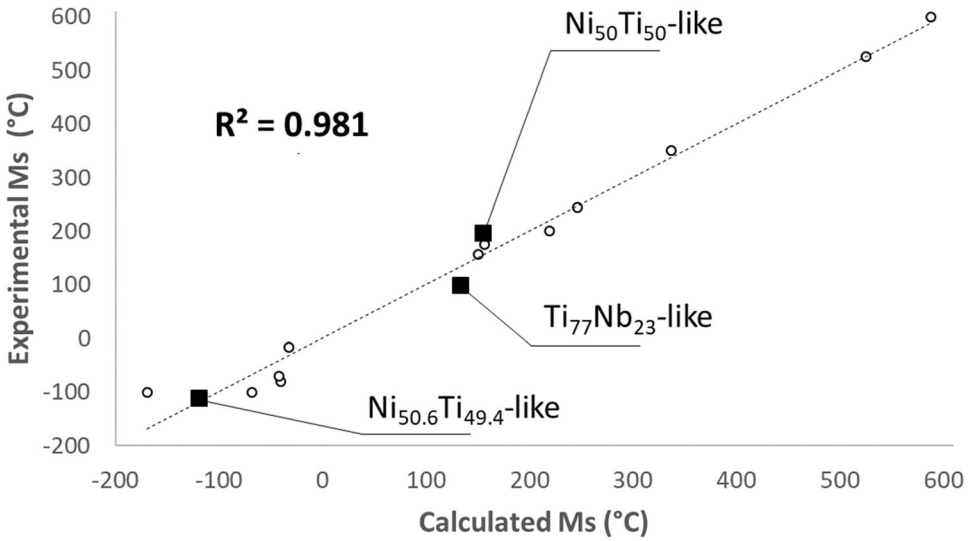

Fig. 3 Correlation curve comparing both temperatures M_s (calculated versus experimental) for the 16 HE-SMAs studied alloys. One can note that the predictions adjust fairly well to a linear function with the experimental values (R^2 = 0.981)

$$(M_s^{calc})_i(^\circ C) = -4.634(Ti)_i + 16.146(Hf)_i + 18.480(Zr)_i - 46.399(Nb)_i - 16.120(Ta)_i + 15.775(Fe)_i - 27.146(Co)_i + 35.265(Al)_i - 24.485(Cu)_i - 0.904(Pd)_i - 13.966(Ni)_i\,(wt.\%) \quad (7)$$

Using the ponderation Eq. (7), 16 values of the M_s^{Calc} temperature are estimated and compared to the 16 values of the M_s^{Exp} temperatures experimentally determined using the DSC technique. Figure 3 shows that Eq. (7) provides estimated values of M_s^{Calc} that are close to M_s^{Exp} (the correlation coefficient R^2 equals 0.981).

It is worth noticing that the M_s temperature calculated for the three investigated HEAs ($Ni_{50}Ti_{50}$-like, $Ni_{50.6}Ti_{49.4}$-like, $Ti_{77}Nb_{23}$-like (at. %)) agree well with the experimental values as evidenced in Fig. 3. This agreement confirms the predictability of the Eq. (7) for NiTi-like and TiNb-like alloys.

Experimental Validation Using Two Manufactured NiTi-like HEAs

As a final experimental validation of the proposed equation, two additional new NiTi-like alloys ($Ti_{16}Hf_{38}Zr_{17}Ni_{19}Cu_{10}$ and $Ti_{16}Hf_{38}Zr_{17}Ni_{19}Cu_5Co_5$ (wt. %)) are fabricated and then investigated in terms of microstructure ensuring the ST state during homogenization heat treatment, as well as a reversible martensite transformation using DSC technique. The latter provides the experimental values of M_s temperature as shown in Fig. 4.

These two alloys have been chosen according to the different criteria proposed in [13] and [19]. The two alloys have been heat-treated to be homogenized and solutioned. Figure 5a and b report the chemical composition data of the two new alloys, the high entropy criterion and the experimental M_s temperatures. These figures show martensite at room temperature on SEM images respectively in the manufactured NiTi-like alloys. $Ti_{16}Hf_{38}Zr_{17}Ni_{19}Cu_{10}$ alloy (wt. %) and $Ti_{16}Hf_{38}Zr_{17}Ni_{19}Cu_5Co_5$ alloy (wt. %) differ only by the partial replacement of Co by Cu for the second alloy. The elements Cu and Co have been chosen because their respective ponderation coefficients in Eq. (7) are comparable.

The first alloy $Ti_{16}Hf_{38}Zr_{17}Ni_{19}Cu_{10}$ (wt. %) corresponds to $Ni_{39.6}Ti_{60.4}$ -like (at. %) whereas the second alloy $Ti_{16}Hf_{38}Zr_{17}Ni_{19}Cu_5Co_5$ (wt. %) corresponds to $Ni_{40}Ti_{60}$-like (at. %).

Knowing the alloying elements of the two new NiTi-like alloys, their M_s temperatures have been estimated using Eq. (7) and compared to the experimentally determined values. The following comparison table (Table 2) summarizes the results:

The difference between the calculated M_s temperature and the experimental one for both HE-SMAs fabricated alloys (Table 2) is 28 °C and 17 °C, respectively. This slight discrepancy is partially due to the uncertainties in the chemical analyses carried out using the SEM investigation technique instead of the spectrometry technique. In fact, it is established that a variation of chemical composition can bring about a deviation in the M_s^{Calc}. For instance, using the Eq. (7), one can assess that an uncertainty of 0.2% in weight of the zirconium (Zr) and the cobalt (Co) produces a variation of M_s^{Calc} of about 10 °C of the $Ti_{16}Hf_{38}Zr_{17}Ni_{19}Cu_5Co_5$ alloy.

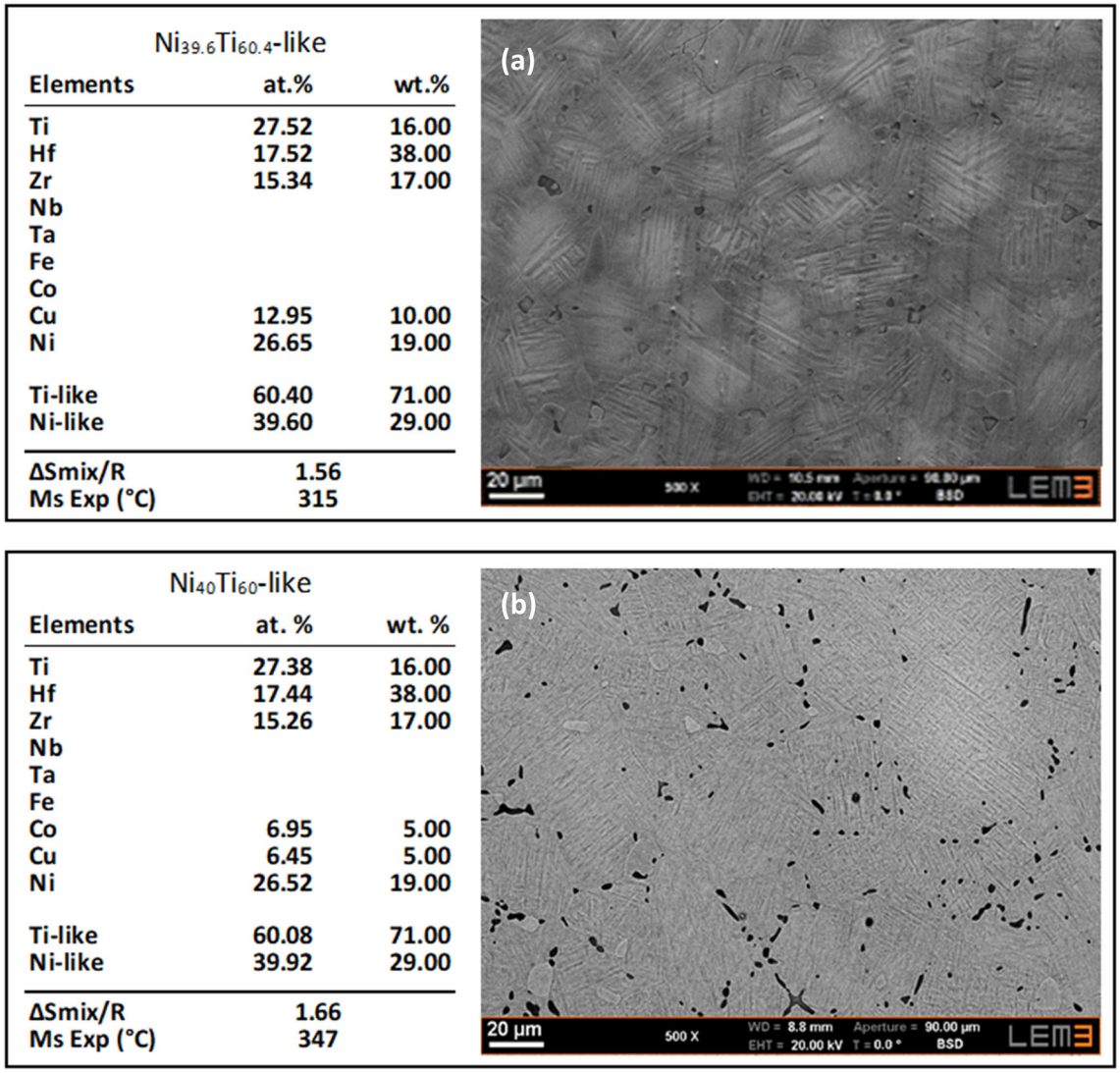

Fig. 4 DSC analyses of $Ni_{39.6}Ti_{60.4}$-like ($Ti_{16}Hf_{38}Zr_{17}Ni_{19}Cu_{10}$) and $Ni_{40}Ti_{60}$-like alloys ($Ti_{16}Hf_{38}Zr_{17}Ni_{19}Cu_5Co_5$)

Conclusion

In this paper, a developed relationship is intended to estimate the martensite transformation temperature (M_s) of HE-SMAs as a function of its chemical weighted composition consisting of the following alloying elements: Al, Co, Cu, Fe, Hf, Nb, Ni, Pd, Ta, Ti, Zr. The ponderation coefficients are extracted from a database of experimental results related to HEAs exhibiting superelastic or shape memory effects. The developed equation has been formulated for HEAs having a metallurgical ST state and a specific mixing entropy (ΔSmix/R) ranging between 1.3 and 1.75. Besides, knowing a target in terms of M_s temperature interval, the proposed equation can be employed to adjust the HE-SMA composition by varying the concentration of some alloying elements in relation to their respective ponderation coefficients.

It must be pointed out that the equivalency elements do not all have the same influence on the M_s temperature of the obtained HEA alloy. Furthermore, it has been demonstrated that when the Cu is partially replaced by Co in the $Ti_{16}Hf_{38}Zr_{17}Ni_{19}Cu_{10}$ alloy, the M_s temperature estimated using the proposed equation has been found in the same range as the M_s estimated experimentally. One can conclude thus that the Co and Cu have almost the same influence on the transformation temperatures from the austenite to the martensite phases (M_s).

The developed approach and the related (M_s) prediction equation can be modified and enriched depending on the interest of the HE-SMAs and the potential other constitutive elements. Indeed, other elements can be added to the composition of the HEA enriching hence the equation. For instance, one can consider the ponderation coefficients of In or Ga but such NiAl-like HE-SMAs have not been

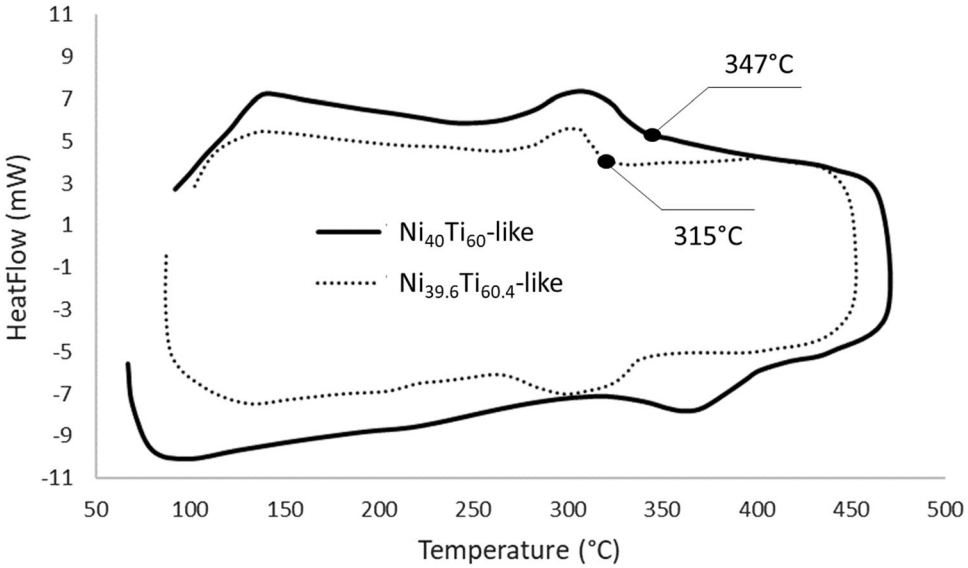

Fig. 5 SEM and XRD analyses of studied alloys: a) $Ni_{40}Ti_{60}$-like alloy, b) $Ni_{39.6}Ti_{60.4}$-like alloy

Table 2 Compositions and transformation temperatures of $Ti_{16}Hf_{38}Zr_{17}Ni_{19}Cu_{10}$ alloy and $Ti_{16}Hf_{38}Zr_{17}Ni_{19}Cu_5Co_5$ alloy (wt. %)

Composition (wt.%)	NiTi-Like (at.%)	M_s^{Calc}(°C)	M_s^{Exp}(°C)
$Ti_{16}Hf_{38}Zr_{17}Ni_{19}Cu_{10}$	$Ni_{39.6}Ti_{60.4}$-like	343	315
$Ti_{16}Hf_{38}Zr_{17}Ni_{19}Cu_5Co_5$	$Ni_{40}Ti_{60}$-like	330	347

extensively studied in the open literature and the related data in terms of M_s have been reported only by Gerstein et al. [20]. It is therefore important to manufacture and produce more HE-SMAs with a similar metallurgical state and ΔSmix/R to enrich the temperature calculation equation and to extend its applicability for other alloying elements.

Acknowledgments This research was supported by the SMART team of the LEM3 laboratory. The authors want to thank sincerely our colleagues Pierre Charbonnier and Jérome Slowensky who provided help that strongly assisted this study.

References

1. Ahlers M (1974) On the stability of the martensite en Béta CuZn alloys. Scr Metall 8:215–216
2. Guilemany JM, Gil FJ (1990) The relationship between chemical composition and transformation temperatures, Ms and As, in poly-crystals and singles-crystals of Cu-Zn-Al shape memory alloys. Thermochim Acta 167:129–138
3. H.Y. KIM, S. Miyazaki 2004 Alternative shape memory alloys. Univ. Tsukuba, Japan 69–85
4. Frenzel J, George EP, Dlouhy A et al (2010) Influence of Ni on martensitic phase transformations in NiTi shape memory alloys. Acta Mater 58:3444–3458. https://doi.org/10.1016/j.actamat.2010.02.019
5. Yaacoub J, Abuzaid W, Brenne F, Sehitoglu H (2020) Superelasticity of (TiZrHf)50Ni25Co10Cu15 high entropy shape memory alloy. Scr Mater 186:43–47. https://doi.org/10.1016/j.scriptamat.2020.04.017
6. Firstov GS, Kosorukova TA, Koval YN, Verhovlyuk PA (2015) Directions for high-temperature shape memory alloys improvement: straight way to high-entropy materials? Shape Mem Superelasticity 1:400–407. https://doi.org/10.1007/s40830-015-0039-7
7. Liu Y, Mccormick PG (1994) Thermodynamic analysis of the martensitic transformation in NiTi. Effect of heat treatment on the transformation behavior. Acta Metall Mater 42:2401–2406
8. Mitwally ME, Farag M (2009) Effect of cold work and annealing on the structure and characteristics of NiTi alloy. Mater Sci Eng A 519:155–166. https://doi.org/10.1016/j.msea.2009.04.057
9. Pattabi M, Murari MS (2014) Effect of cold rolling on phase transformation temperatures of NiTi shape memory alloy. J Mater Eng Perform. https://doi.org/10.1007/s11665-014-1344-6
10. ASTM F 2004 2008 Standard Test Method for Transformation Temperature of Nickel-Titanium Alloys by Thermal Analysis
11. Piorunek D, Frenzel J, Niels J et al (2020) Intermetallics chemical complexity, microstructure and martensitic transformation in high entropy shape memory alloys. Intermetallics. https://doi.org/10.1016/j.intermet.2020.106792
12. Firstov GS, Kosorukova TA, Koval YN, Odnosum VV (2015) High Entropy shape memory alloys. Mater Today Proc 2:S499–S503. https://doi.org/10.1016/j.matpr.2015.07.335
13. Peltier L, Lohmuller P, Meraghni F et al (2020) Investigation and composition characterization of a "NiTi-like" alloy combining high temperature shape memory and high entropy. Shape Mem Superelasticity. https://doi.org/10.1007/s40830-020-00290-2
14. Canadinc D, Trehern W, Ma J et al (2019) Ultra-high temperature multi-component shape memory alloys. Scr Mater 158:83–87. https://doi.org/10.1016/j.scriptamat.2018.08.019
15. Wang L, Fu C, Wu Y et al (2019) Superelastic effect in Ti-rich high entropy alloys via stress-induced martensitic transformation. Scr Mater 162:112–117. https://doi.org/10.1016/j.scriptamat.2018.10.035
16. Li S, Cong D, Sun X et al (2019) Wide-temperature-range perfect superelasticity and giant elastocaloric effect in a high entropy

alloy. Mater Res Lett. https://doi.org/10.1080/21663831.2019.1659436
17. Piorunek D, Oluwabi O, Frenzel J et al (2020) Effect of off-stoichiometric compositions on microstructures and phase transformation behavior in Ni-Cu-Pd-Ti-Zr-Hf high entropy shape memory alloys. J Alloys Compd. https://doi.org/10.1016/j.jallcom.2020.157467
18. Christian H, Khemais B, Jan S et al (2020) The Effect of increasing chemical complexity on the mechanical and functional behavior of NiTi-related shape memory alloys. Shape Mem Superelasticity. https://doi.org/10.1007/s40830-020-00284-0
19. Peltier L, Berveiller S, Meraghni F et al (2021) Martensite transformation and superelasticity at high temperature of (TiHfZr)74(NbTa)26 high-entropy shape memory alloy. Shape Mem Superelasticity. https://doi.org/10.1007/s40830-021-00323-4
20. Gerstein G, Firstov GS, Kosorukova TA et al (2018) Development of B2 shape memory intermetallics beyond NiAl, CoNiAl and CoNiGa. Shape Mem Superelasticity 4:360–368. https://doi.org/10.1007/s40830-018-0180-1
21. Zhang C, Zhu C, Harrington T et al (2018) multifunctional non-equiatomic high entropy alloys with superelastic, high damping, and excellent cryogenic properties. Adv Eng Mater 1800941:1–9. https://doi.org/10.1002/adem.201800941
22. Karaduman O, Özkul İ, Altın S et al (2018) New Cu-al based quaternary and quinary high temperature shape memory alloy composition systems. AIP Conf Proc. https://doi.org/10.1063/1.5078902
23. Chumlyakov YI, Kireeva IV, Kuksgauzen IV et al (2020) Superelasticity and shape memory effect under tension and compression in the [001]-oriented single crystals of non-equiatomic Fe-Ni-Co-Al-Ti high-entropy alloy. Russ Phys J 62:126–133. https://doi.org/10.1007/s11182-020-01980-1
24. Abuzaid W, Sehitoglu H (2018) Superelasticity and functional fatigue of single crystalline FeNiCoAlTi iron-based shape memory alloy. Mater Des 160:642–651. https://doi.org/10.1016/j.matdes.2018.10.003
25. Belkahla S, Zufiiga HF, G G, (1993) Elaboration and characterization of new low temperature shape memory Cu-Al-Be alloys. Mater Sci Eng A 169:119–124
26. Peltier L, Olivier P, Patrick M, et al 2021 Production and mechanical properties of Cu-Al-Ni-Be shape memory alloy thin ribbons using a cold co-rolled process. J: Shape Mem Superelasticity 7(2): 344-352
27. Recarte V, Pérez-Sáeza R, Bocanegra E et al (1999) Dependence of the martensitic transformation characteristics on concentration in Cu–Al–Ni shape memory alloys. Mater Sci Eng A. https://doi.org/10.1016/S0921-5093(99)00302-0
28. Peltier L, Lohmuller P, Meraghni F et al (2020) Investigation and composition characterization of a "NiTi-like" alloy combining high temperature shape memory and high entropy. Shape Mem Superelasticity 6:273–283. https://doi.org/10.1007/s40830-020-00290-2
29. Guo S, Liu CT (2011) Phase stability in high entropy alloys: formation of solid-solution phase or amorphous phase. Prog Nat Sci Mater Int 21:433–446. https://doi.org/10.1016/S1002-0071(12)60080-X
30. Yeh J (2006) Recent progress in high entropy alloys. Ann Chim Sci Mat 31:633–648
31. Chen CH, Chen YJ (2019) Shape memory characteristics of (TiZrHf)50Ni25Co10Cu15 high entropy shape memory alloy. Scr Mater 162:185–189. https://doi.org/10.1016/j.scriptamat.2018.11.023
32. Chang S, Lin P, Tsai C (2019) High-temperature martensitic transformation of CuNiHfTiZr high- entropy alloys. Sci Rep. https://doi.org/10.1038/s41598-019-55762-y
33. W. Fred Ramirez 1998 Computational Methods for Process Simulation, 2nd ed